C60 Bioconjugation with Proteins: Towards a Palette of Carriers for All pH Ranges

Matteo Di Giosia [1],*, Francesco Valle [2], Andrea Cantelli [1], Andrea Bottoni [1], Francesco Zerbetto [1] and Matteo Calvaresi [1],*

[1] Dipartimento di Chimica "G. Ciamician", Università di Bologna, via F. Selmi 2, 40126 Bologna, Italy; a.cantelli@unibo.it (A.C.); andrea.bottoni@unibo.it (A.B.); francesco.zerbetto@unibo.it (F.Z.)
[2] Istituto per lo Studio dei Materiali Nanostrutturati (CNR-ISMN), Consiglio Nazionale delle Ricerche, via P. Gobetti 101, 40129 Bologna, Italy; f.valle@ismn.cnr.bo.it
* Correspondence: matteo.digiosia2@unibo.it (M.D.G.); matteo.calvaresi3@unibo.it (M.C.)

Abstract: The high hydrophobicity of fullerenes and the resulting formation of aggregates in aqueous solutions hamper the possibility of their exploitation in many technological applications. Noncovalent bioconjugation of fullerenes with proteins is an emerging approach for their dispersion in aqueous media. Contrary to covalent functionalization, bioconjugation preserves the physicochemical properties of the carbon nanostructure. The unique photophysical and photochemical properties of fullerenes are then fully accessible for applications in nanomedicine, sensoristic, biocatalysis and materials science fields. However, proteins are not universal carriers. Their stability depends on the biological conditions for which they have evolved. Here we present two model systems based on pepsin and trypsin. These proteins have opposite net charge at physiological pH. They recognize and disperse C60 in water. UV-Vis spectroscopy, zeta-potential and atomic force microscopy analysis demonstrates that the hybrids are well dispersed and stable in a wide range of pH's and ionic strengths. A previously validated modelling approach identifies the protein-binding pocket involved in the interaction with C60. Computational predictions, combined with experimental investigations, provide powerful tools to design tailor-made C60@proteins bioconjugates for specific applications.

Keywords: fullerenes; nanohybrids; nanobiotechnology; bioconjugation; chemical stability

1. Introduction

C60, the most representative member of the fullerenes family, has steadily attracted interest for its possible use in various fields, including nanomedicine [1–7]. A plethora of fullerene-based compounds have been synthesized with different targets. They display a range of biological activities that are potentially useful in anticancer therapy, antimicrobial therapy, enzyme inhibition, controlled drug delivery, and contrast or radioactivity-based diagnostic imaging [7–13]. Noteworthy is the possibility of their use in photodynamic and photothermal therapies [8,14,15]. The photophysical and electrochemical properties of C60 depend on their dispersion and a strict control of their disaggregation is truly necessary for nanotechnological applications [16–18]. To date two main approaches have been followed to tackle fullerene insolubility in water:

(i) the covalent approach is the most used method to prevent fullerene aggregation. The benefits obtained by functionalization are often offset by reduced photophysical performances [19];

(ii) the noncovalent approach requires the use of supramolecular hosts that are amphipathic molecules able to interact with a single fullerene and to screen it from the aqueous environment. A variety of hosts is capable of interacting with fullerenes. They include surfactants, synthetic polymers, biopolymers, cyclodextrin [20], to name a few. In all cases, they stabilize small clusters

of fullerenes [21]. In recent years, also proteins have become used as dispersing agents of fullerenes [9,22–24], CNTs [25–29] and graphene [30]. Proteins are naturally amphiphilic. This feature may avoid complicated synthetic procedures or the use of organic solvents. Most proteins are also pH responsive, which is an advantage for some manipulations [26]. Steric hindrance and electrostatic repulsion are the key factors determining the stability of the dispersion of carbon nanomaterials-protein complexes in aqueous solutions [31].

Protein corona [32–34] determines the biological fate of ultra-small NPs and nanoclusters and controls physiological responses. From the biological point of view, encapsulation of fullerenes by proteins may control and possibly decrease the cytotoxicity. Well-dispersed fullerenes [35] and CNTs are less toxic than their agglomerates [36]. Protein binding can also alter the cellular pathways of interaction with carbon nanomaterials. Ultimately, coating of carbon nanomaterials with proteins can confer them a new biological identity [37].

We recently proposed the use of lysozyme to disperse with a 1:1 stoichiometry C_{60} in water [23]. The hybrid is well-defined and the fullerene binds selectively in the protein-substrate binding pocket. The protein-based supramolecular adduct preserves the photophysical properties of C_{60} and allows the exploitation of C_{60} as a photosensitizer for photodynamic treatments [35].

In this work, we show that the non-covalent bioconjugation of C_{60} with proteins offers a palette of carriers for fullerenes for all pH ranges. We evaluate the stability of C_{60}@protein complexes in biologically relevant conditions. Two proteins characterized by opposite net charges in physiological conditions are used as model systems and the role of the electrostatic contribution to the stability of their adducts with C_{60} is identified. Applications of docking protocols and Molecular Mechanics Poisson–Boltzmann Surface Area (MMPBSA) calculations [38,39] further provide accurate description of the C_{60} binding pocket involved in the interaction between protein and C_{60}.

2. Materials and Methods

Trypsin from porcine pancreas (Cat. no. T0303), pepsin from porcine gastric mucosa (Cat. no. P7012), fullerene C_{60} (Cat. no. 483036) were purchased from Sigma Aldrich. They were used without further purifications. Phosphate-buffered saline (PBS) solutions were prepared dissolving the tablets purchased from Sigma Aldrich (Cat. no. P4417) in milli-Q ultrapure water.

2.1. C_{60}@Protein Synthesis

The C_{60}@protein hybrids were prepared mixing an excess of fullerene powder with a 0.3 mM solution of each protein (5 mL), with a 2:1 stoichiometry. NaOH and HCl 1M were used to adjust pH of the protein solutions. The heterogeneous mixtures were then sonicated in a vial for 120 min using a probe tip ultrasonicator (Ultrasonic Processor UP200St, Hielscher Ultrasonics GmbH, Teltow, Germany), equipped with a sonotrode S26d7, used at 40% of the maximum amplitude). During the process, the sample was refrigerated with an ice bath. The dark brown turbid mixture obtained after the sonication was centrifuged at 10 kRCF. The resulting supernatant was then collected and characterized.

2.2. C_{60}@Protein Characterization

UV-Vis absorption spectra were recorded at 25 °C by means of Cary 60 UV-Vis Spectrophotometer (Agilent, Santa Clara, CA, USA). Surface charge analysis of the hybrids were estimated measuring the zeta-potential at 25 °C by means of Malvern Nano ZS.

Atomic Force Microscopy (AFM) experiments were performed at the SPM@ISMN microscopy facility in Bologna. AFM analysis were done with a Multimode VIII equipped with a Nanoscope V controller (Bruker Nano Surface, Santa Barbara, CA, USA) operated in ScanAsyst mode to evaluate the quality of the monodispersion of the bioconjugates. The samples were prepared by drop casting 10 μL of C_{60}@protein solution onto a freshly cleaved mica substrate for 10 min then rinsed with milli-Q ultrapure water and dried under a nitrogen stream.

2.3. Computational Protocol

Generation of the poses. Docking models were obtained using the PatchDock algorithm [40]. PatchDock takes as input two molecules and computes three-dimensional transformations of one of the molecules with respect to the other with the aim of maximizing surface shape complementarity, while minimizing the number of steric clashes.

Scoring of the poses. Accurate rescoring of the complexes is then carried out using FireDock program [41]. This method simultaneously targets the problem of flexibility and scoring of solutions produced by fast rigid-body docking algorithms. Sidechain flexibility is modeled by rotamers and Monte Carlo minimization [42]. Following the rearrangement of the side-chains, the relative position of the docking partners is refined by Monte Carlo minimization of the binding score function. Free energy of solvation/desolvation in the binding process is taken into account by a solvation model that uses estimated effective atomic contact energies (ACE) [43]. All the candidates are ranked by a binding score [43]. This score includes, in addition to atomic contact energy used to estimate the desolvation energies [43], van der Waals interactions, partial electrostatics, explicit hydrogen and disulfide bonds contribution. In addition, three components to the total binding score are added: $E_{\pi\text{-}\pi}$ for the calculation of the π-π interactions, $E_{cation\text{-}\pi}$ for the calculation of the cation-π interactions and E_{aliph} for the calculation of hydrophobic interactions.

Minimizing the pose. The best poses for every selected protein were full minimized by AMBER 12 [44]. The ff12SB force field [44] was used to model the proteins, while the fullerene atoms were modeled as uncharged Lennard-Jones particles by using the CA atom type (sp^2 Aromatic Carbon parameter), also from the AMBER force field. The minimization was carried out with sander, using the GB (Generalized Born) model [45] for the solvation and no cut-off for van der Waals and electrostatic was used.

MM-GBSA analysis. In order to identify the residues responsible for the binding of the proteins to C_{60}, we carried out a decomposition analysis of the optimized structure according to the MM-GBSA scheme [38,39]. The per-residue decomposition analysis provides the contribution of the individual amino acids to the binding.

3. Results and Discussions

The ability of C_{60} to interact with proteins is a recent subject of investigation. Collectively, van der Waals, hydrophobic and electrostatic interactions must cooperate to establish energetically favorable interactions between a protein and a fullerene in order to allow the formation of a stable complex [46]. Geometrical complementarity also plays a primary role to maximize the effect of the stabilizing contributes [47]. Crucial for the understanding of protein-fullerene interactions is the identification of the fullerene-binding site together with the possible subsequent proteins structural modification [48]. It should also be further assessed if the interaction occurs between a single fullerene with a single protein or if fullerenes clusters are surrounded by a number of proteins.

Pepsin (pI = 2.2 – 3) [49] and trypsin (pI = 10.2 – 10.8) [50] are proteins characterized by very different values of isoelectric point, which makes one negatively and the other positively charged in physiological conditions. Sonication of C_{60} with each protein was performed in acidic (pH 2), neutral, and basic pH (pH 12) of unbuffered aqueous solutions, to avoid stabilizing/destabilizing effects due to the different buffer composition. Pepsin was able to disperse fullerene in water only at basic pH, where the protein is negatively charged, while trypsin showed the best performances at acidic pH.

The two batches of hybrids were synthetized under optimized conditions. After sonication and centrifugation, the supernatants were collected and characterized. UV-Vis spectra of the solutions (Figure 1) show the diagnostic absorption bands of C_{60} at 341 nm and the overlap of C_{60} and protein absorption bands between 260 and 290 nm. Based on the extinction coefficients of both components of the adducts [51], the absorption spectra suggest a 1:1 stoichiometry between C_{60} and trypsin, while 1:2 stoichiometry can be estimated for the C_{60} and pepsin complex. UV-Vis spectra also suggest that the presence of particle aggregates, observed prior to centrifugation, was completely removed since scattering is not exhibited.
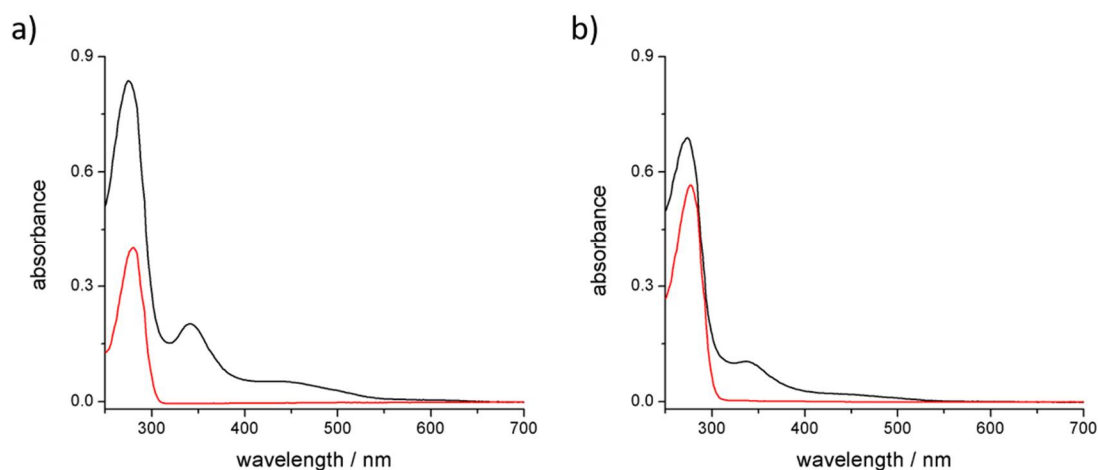
Figure 1. UV-visible spectra of (**a**) C_{60}@trypsin (black line) and trypsin (red line); (**b**) C_{60}@pepsin (black line) and pepsin (red line).

3.1. C_{60}@Pepsin — C_{60}@trypsin, an Atomistic View

Surface complementarity between the proteins and the C_{60} surface appears. The results of the docking protocol explain the stoichiometry observed by the UV-visible spectra. Pepsin is characterized by a dimeric interface region. In this region, two fullerene binding pockets are identifiable (Figure 2a,b).
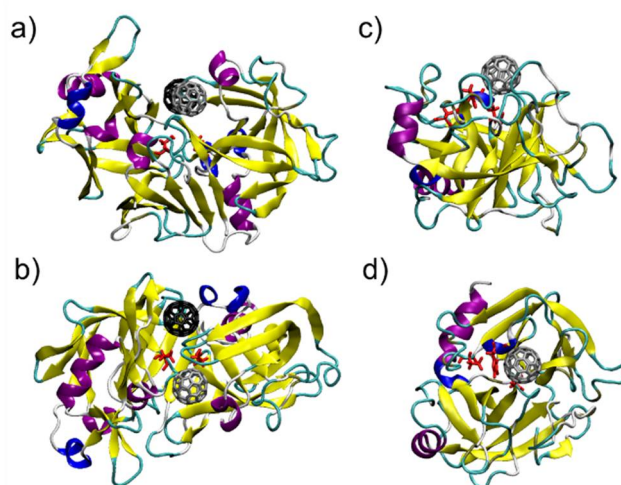
Figure 2. Two perspectives of C_{60}@pepsin (**a**,**b**) grey coloured C_{60} occupies the binding pocket 1, black coloured C_{60} occupies the binding pocket 2 and C_{60}@trypsin (**c**,**d**). In red, the catalytic residues of the two proteins.

The binding between C_{60} and pepsin is not surprising, since pepsin is an aspartic protease and structurally strongly correlates to HIV protease: fullerenes are well known inhibitors of HIV-1 protease [52–55]. In pepsin, as in the HIV protease, fullerenes block the large active site groove [52–55]. C_{60} is also a known serine protease inhibitor [56], and in fact C_{60} binds in the trypsin active site: a single, well defined binding pocket is identified by the docking protocol in this region (Figure 2c,d). For the two C_{60}@protein hybrids tested here, MM-GBSA analysis of the structures in their optimized geometries provides a quantitative description of the C_{60} binding pocket and identifies the more effectively interacting residues. Table 1 shows the 10 largest interactions between the residues of the proteins and C_{60}. The three most interacting residue for binding pocket are represented in Figure 3a–c.

Table 1. Interaction energies (kcal mol^{-1}) of the top 10 residues interacting with C$_{60}$.

C$_{60}$@protein Complex	Top 10 Residues Interacting with C$_{60}$				
C$_{60}$@Pepsin-Binding pocket 1	Phe 111 = −5.7	Leu 112 = −3.1	Thr 218 = −3.0	Ser 219 = −2.9	Thr 12 = −2.8
	Glu 13 = −2.8	Phe 117 = −2.6	Ile 30 = −2.5	Tyr 75 = −2.5	Thr 77 = −2.2
C$_{60}$@Pepsin-Binding pocket 2	Val 291 = −4.9	Thr 74 = −4.3	Pro 292 = −3.7	Tyr 75 = −3.4	Gly 76 = −2.7
	Met 289 = −1.4	Thr 293 = −1.3	Tyr 189 = −1.2	Asp 290 = −1.0	Leu 298 = −0.6
C$_{60}$@Trypsin	His 57 = −4.9	Phe 41 = −4.2	Gln 192 = −3.5	Cys 58 = −3.4	Cys 42 = −2.7
	Gly 193 = −1.8	Ser 195 = −1.7	Asp 194 = −0.8	Tyr 151 = −0.6	Leu 99 = −0.4
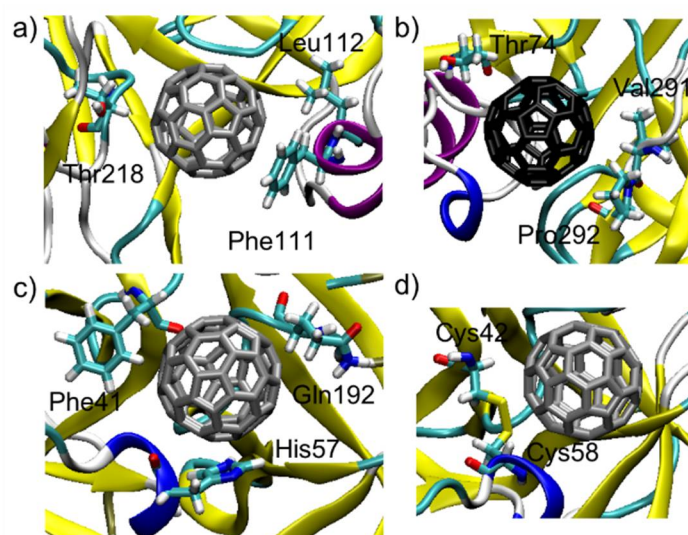
Figure 3. Top 3 residues interacting with C$_{60}$ in the (**a**) pepsin binding pocket 1; (**b**) pepsin binding pocket 2; (**c**) Top 3 residues interacting with the C$_{60}$ in the trypsin binding pocket; (**d**) Interaction in the trypsin binding pocket between C$_{60}$ and a disulfide bridge (Cys42-Cys58).

From Table 1, Figure 3, and Figures S1–S3 it appears that proteins are able to interact with C$_{60}$ via:

(i) π-π stacking interactions that are established between aromatic residues (phenylalanine, tyrosine, histidine) and C$_{60}$ surface [25,57];

(ii) Hydrophobic interactions (leucine, isoleucine, methionine, proline, glycine) that are established in water between aliphatic residues and C$_{60}$ surface [25];

(iii) Surfactant-like interactions where amphiphilic residues (threonine, serine, aspartate) behave similarly to surfactants and solvate C$_{60}$. The hydrophobic aliphatic chains of these residues interact with C$_{60}$ surface, whereas the hydrophilic groups point out toward water [25,58,59].

In the case of trypsin, of interest is the interaction between a disulfide bridge (Cys42-Cys58) and C$_{60}$ (Figure 3d). This kind of interaction was recently highlight by Hirano and coworkers for carbon nanotubes [60,61].

3.2. AFM Analysis of C$_{60}$@Protein Hybrids

UV-Vis spectra and molecular modelling exhibit the expected stoichiometry between C$_{60}$ and proteins. They do not give information about the possible aggregation of the adducts. Atomic force microscopy is a direct technique to evaluate the size distribution of particles.

In Figure 4a, the C$_{60}$@trypsin hybrids are monomoleculary dispersed when deposited on a negatively charged mica surface. C$_{60}$@trypsin is positively charged; hence, an electrostatic interaction takes place with the surface. The height distribution (Figure 4c) of both C$_{60}$@trypsin and the trypsin reference (obtained in the same conditions) shows an average height which is slightly lower than the expected value. This behavior is a consequence of the strong electrostatic interaction, which squashes

the proteins over the surface in order to maximize the attractive electrostatic contacts. Conversely, negatively charged pepsin hybrid (Figure 4f) shows an average height, which is slightly higher than the average size of the protein. These results mainly originate from the combination of different forces: (i) the pepsin tendency to self-associate; (ii) the electrostatic repulsion between the pepsin and the surface, which reduces the number of interactions, as confirmed also by the small number of the particles deposited on the mica which repels the adduct.

The AFM analysis demonstrates the absence of C_{60}@proteins aggregates, or nC_{60} clusters dispersed by the proteins.
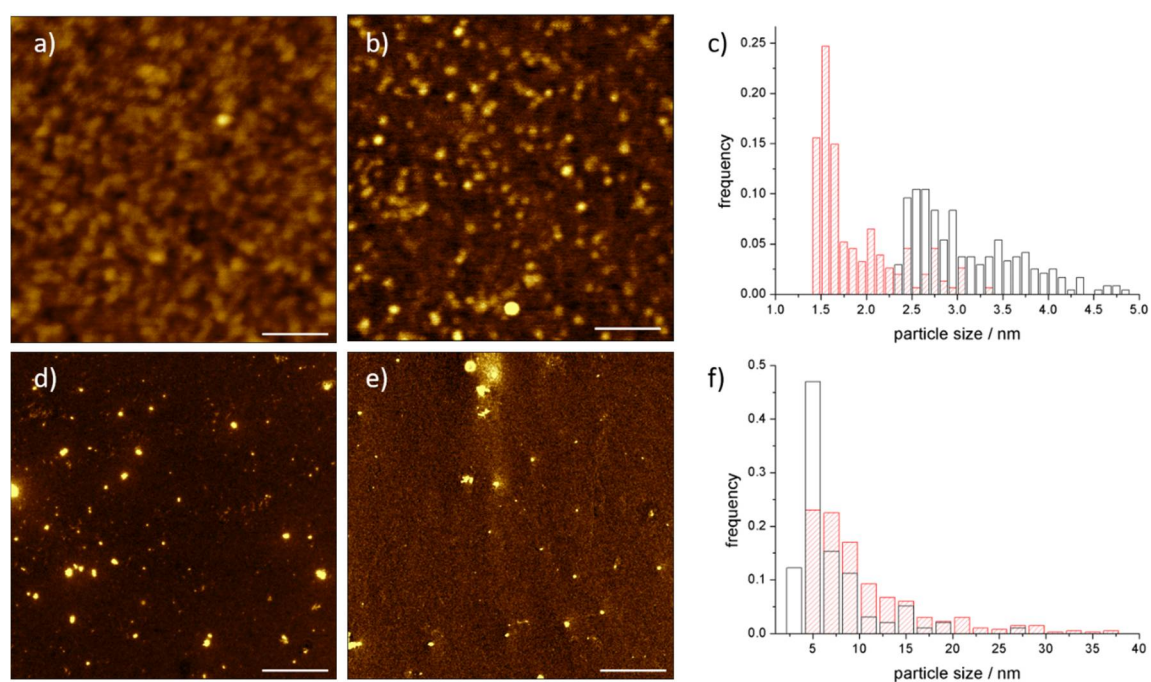
Figure 4. AFM images of (**a**) C_{60}@trypsin; (**b**) trypsin and (**c**) height distribution of C_{60}@trypsin (red) and trypsin (black). AFM images of (**d**) C_{60}@pepsin, (**e**) pepsin and (**f**) height distribution of C_{60}@pepsin (red) and pepsin (black). Scale bar (**a,b**) 100 nm; (**d,e**) 1 μm.

3.3. Stability of the Complex in Aqueous Media

Compared to the chemical functionalization of the fullerenes, one of the advantages from the use of host-guest system is the possibility to tune the stability of the complex in aqueous media. The tuning can be achieved by acting only on the host system, which is the protein. Evaluating the behavior of C_{60}@proteins at different pH's and physiological conditions, it was found that the stability of the hybrid in aqueous media was completely governed by the protein. To understand if proteins pH sensitivity was retained, acid-basic titration was performed. Zeta potential and UV-Vis spectra were obtained. The correlation between zeta potential and pH gives information about the behavior of the complex for possible future in vivo experiments, since pH varies in different compartments of the organisms. Moreover, the greater the range of pH stability the wider the conditions for subsequent manipulation of the adduct. pH dependent zeta potential trends of C_{60}@trypsin and C_{60}@pepsin are shown in Figure 5.
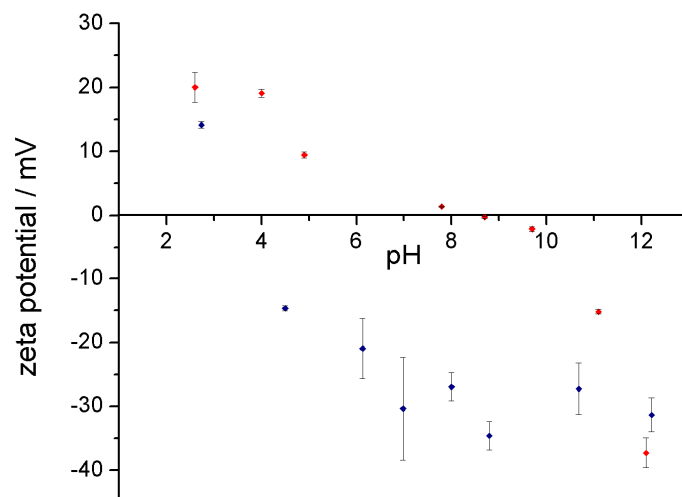
Figure 5. Zeta potential of C$_{60}$@trypsin (in red) and C$_{60}$@pepsin (in blue) hybrids as a function of the pH in aqueous solution. Standard deviations are shown in the error bars.

The isoelectric points (IEP) of both adducts resulted slightly shifted to values of pH's closer to neutrality with respect to IEP of the pristine proteins. This phenomenon can be attributed to a reduced accessibility to pH sensitive groups upon fullerene complexation. A further effect is related to the local change of the environment polarity, which could slightly perturb the pKa of few charged residues. Electrostatic repulsion and steric hindrance are two of the major mechanisms active in the dispersion of fullerene in protein solutions. At pH values different from the isoelectric point (IEP), the charge distribution on the atoms of the proteins makes the protein-stabilized C$_{60}$ repel each other. For pH values closer to the IEP, the electrostatic repulsion between the proteins/adducts becomes minimal. The stability of possible aggregates is governed only by steric hindrance.

For C$_{60}$@pepsin complexes at pH values close to IEP (2.7 and 4.5), aggregation phenomena occurred after few minutes. C$_{60}$@trypsin complexes did not aggregate also for pH values close to the IEP. Around the IEP, for C$_{60}$@trypsin, protein steric repulsion provides a barrier to prevent fullerene aggregation. The maximum stability for individual C$_{60}$@pepsin complexes was obtained in neutral and basic conditions. Absorption spectra performed on the same samples did not show changes of shape and intensity (Figure 6) between the different samples. After three months, C$_{60}$@pepsin is perfectly stable while for C$_{60}$@trypsin, more than 90% of the initial dispersed fullerene is detected (Figure S4).
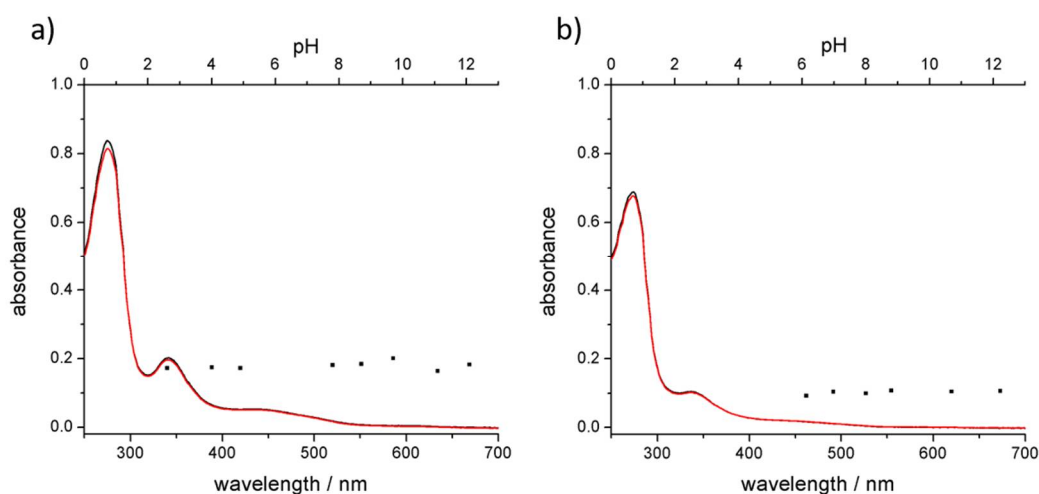
Figure 6. UV-Vis absorption spectra of (**a**) C$_{60}$@trypsin and (**b**) C$_{60}$@pepsin in water (black lines) and PBS (red lines). Black dots represent the absorbance of fullerene diagnostic band (341 nm) of the hybrids at different pH values (top axis).

Comparison of the absorption spectra of C_{60}@trypsin (Figure 6a) and C_{60}@pepsin (Figure 6b) in water and phosphate-buffered saline solution shows that the hybrids are stable also in physiologically relevant conditions (represented by PBS). This is an important difference with other C_{60} adducts, for instance fullerenes dispersed by cyclodextrins rapidly precipitates when NaCl is added [62]. On the opposite, proteins are stable in a "salty environment" that represents their physiological condition.

These results suggest that fine-tuning of the net charge of the complex is possible and therefore it should also be possible to take advantage of the nature of each protein to create optimal C_{60}-protein systems as a function of the pH. Tuning the net charge of the protein used to host the C_{60} molecule it is possible to governs its interactions with cellular and bacterial surface, controlling C_{60} toxicity [63–66].

Supplementary Materials: Supplementary materials can be found at www.mdpi.com/xxx/s1.

Author Contributions: Synthesis and characterization of C_{60}@proteins A.C. and M.D.G.; AFM Measurements and Data Analysis, F.V. and M.D.G.; Computational Analysis, M.C., A.B. and F.Z.; Conceptualization, Methodology M.C.; Funding Acquisition, M.C. All authors contributed to the analysis of the results and the writing of the manuscript.

Acknowledgments: This study was supported by the Italian Ministry of Education, University and Research MIUR-SIR Programme no. RBSI149ZN9-BIOTAXI funded to M.C.

Conflicts of Interest: The authors declare no conflict of interest

References

1. Nakamura, E.; Isobe, H. Functionalized fullerenes in water. The First 10 years of their chemistry, Biology, and Nanoscience. *Acc. Chem. Res.* **2003**, *36*, 807–815, doi:10.1021/AR030027Y.

2. Goodarzi, S.; Da Ros, T.; Conde, J.; Sefat, F.; Mozafari, M. Fullerene: Biomedical engineers get to revisit an old friend. *Mater. Today* **2017**, *20*, 460–480, doi:10.1016/J.MATTOD.2017.03.017.

3. Castro, E.; Garcia, A.H.; Zavala, G.; Echegoyen, L. Fullerenes in biology and medicine. *J. Mater. Chem. B* **2017**, *5*, 6523–6535, doi:10.1039/C7TB00855D.

4. Dellinger, A.; Zhou, Z.; Connor, J.; Madhankumar, A.; Pamujula, S.; Sayes, C.M.; Kepley, C.L. Application of fullerenes in nanomedicine: An update. *Nanomedicine* **2013**, *8*, 1191–1208, doi:10.2217/nnm.13.99.

5. Partha, R.; Conyers, J.L. Biomedical applications of functionalized fullerene-based nanomaterials. *Int. J. Nanomedicine* **2009**, *4*, 261–275, doi:10.2147/IJN.S5964.

6. Bosi, S.; Da Ros, T.; Spalluto, G.; Prato, M. Fullerene derivatives: An attractive tool for biological applications. *Eur. J. Med. Chem.* **2003**, *38*, 913–923.

7. Montellano, A.; Da Ros, T.; Bianco, A.; Prato, M. Fullerene C60 as a multifunctional system for drug and gene delivery. *Nanoscale* **2011**, *3*, 4035–4041, doi:10.1039/c1nr10783f.

8. Mroz, P.; Tegos, G.P.; Gali, H.; Wharton, T.; Sarna, T.; Hamblin, M.R. Fullerenes as photosensitizers in photodynamic therapy. In *Medicinal Chemistry and Pharmacological Potential of Fullerenes and Carbon Nanotubes. Carbon Materials: Chemistry and Physics*; Springer: Dordrecht, Netherlands, 2008; pp. 79–106.

9. Calvaresi, M.; Zerbetto, F. Baiting proteins with C60. *ACS Nano* **2010**, *4*, 2283–2299, doi:10.1021/nn901809b.

10. Yang, S.-T.; Wang, H.; Guo, L.; Gao, Y.; Liu, Y.; Cao, A. Interaction of fullerenol with lysozyme investigated by experimental and computational approaches. *Nanotechnology* **2008**, *19*, 395101, doi:10.1088/0957-4484/19/39/395101.

11. Chaudhuri, P.; Paraskar, A.; Soni, S.; Mashelkar, R.A.; Sengupta, S. Fullerenol–Cytotoxic conjugates for cancer chemotherapy. *ACS Nano* **2009**, *3*, 2505–2514, doi:10.1021/nn900318y.

12. Bolskar, R.D. Gadolinium endohedral metallofullerene-based MRI contrast agents. In *Medicinal Chemistry and Pharmacological Potential of Fullerenes and Carbon Nanotubes. Carbon Materials: Chemistry and Physics*; Springer: Dordrecht, Netherlands, 2008; pp. 157–180.

13. Da Ros, T. Twenty years of promises: Fullerene in medicinal chemistry In *Medicinal Chemistry and Pharmacological Potential of Fullerenes and Carbon Nanotubes. Carbon Materials: Chemistry and Physics*; Springer: Dordrecht, Netherlands, 2008; pp. 1–21.

14. Sharma, S.K.; Chiang, L.Y.; Hamblin, M.R. Photodynamic therapy with fullerenes in vivo: Reality or a dream? *Nanomedicine* **2011**, *6*, 1813–1825, doi:10.2217/nnm.11.144.

15. Mroz, P.; Tegos, G.P.; Gali, H.; Wharton, T.; Sarna, T.; Hamblin, M.R. Photodynamic therapy with fullerenes. *Photochem. Photobiol. Sci.* **2007**, *6*, 1139–1149, doi:10.1039/b711141j.

16. Guldi, D.M.; Hungerbuehler, H.; Asmus, K.-D. Redox and excitation studies with C60-substituted malonic acid diethyl esters. *J. Phys. Chem.* **1995**, *99*, 9380–9385, doi:10.1021/j100023a013.

17. Guldi, D.M.; Prato, M. Excited-state properties of C60 fullerene derivatives. *Acc. Chem. Res.* **2000**, *33*, 695–703, doi:10.1021/AR990144M.

18. Verma, M.L.; Naebe, M.; Barrow, C.J.; Puri, M. Enzyme immobilisation on amino-functionalised multi-walled carbon nanotubes: Structural and biocatalytic characterisation. *PLoS One* **2013**, *8*, e73642, doi:10.1371/journal.pone.0073642.

19. Hamano, T.; Okuda, K.; Mashino, T.; Hirobe, M.; Arakane, K.; Ryu, A.; Mashiko, S.; Nagano, T. Singlet oxygen production from fullerene derivatives: Effect of sequential functionalization of the fullerene core. *Chem. Commun.* **1997**, 21–22, doi:10.1039/a606335g.

20. Ikeda, A. Water-soluble fullerenes using solubilizing agents, and their applications. *J. Incl. Phenom. Macrocycl. Chem.* **2013**, *77*, 49–65, doi:10.1007/s10847-013-0319-9.

21. Dallavalle, M.; Leonzio, M.; Calvaresi, M.; Zerbetto, F. Explaining fullerene dispersion by using micellar solutions. *ChemPhysChem* **2014**, *15*, 2998–3005, doi:10.1002/cphc.201402282.

22. Vance, S.J.; Desai, V.; Smith, B.O.; Kennedy, M.W.; Cooper, A. Aqueous solubilization of C60 fullerene by natural protein surfactants, latherin and ranaspumin-2. *Biophys. Chem.* **2016**, *214–215*, 27–32, doi:10.1016/J.BPC.2016.05.003.

23. Calvaresi, M.; Arnesano, F.; Bonacchi, S.; Bottoni, A.; Calò, V.; Conte, S.; Falini, G.; Fermani, S.; Losacco, M.; Montalti, M.; Natile, G.; Prodi, L.; Sparla, F.; Zerbetto, F. C60@Lysozyme: Direct observation by nuclear magnetic resonance of a 1:1 fullerene protein adduct. *ACS Nano* **2014**, *8*, 1871–7, doi:10.1021/nn4063374.

24. Calvaresi, M.; Zerbetto, F. Fullerene sorting proteins. *Nanoscale* **2011**, *3*, 2873–2881, doi:10.1039/c1nr10082c.

25. Calvaresi, M.; Zerbetto, F. The devil and holy water: Protein and carbon nanotube hybrids. *Acc. Chem. Res.* **2013**, *46*, 2454–2463, doi:10.1021/ar300347d.

26. Nepal, D.; Geckeler, K.E. pH-Sensitive dispersion and debundling of single-walled carbon nanotubes: Lysozyme as a tool. *Small* **2006**, *2*, 406–412, doi:10.1002/smll.200500351.

27. Matsuura, K.; Saito, T.; Okazaki, T.; Ohshima, S.; Yumura, M.; Iijima, S. Selectivity of water-soluble proteins in single-walled carbon nanotube dispersions. *Chem. Phys. Lett.* **2006**, *429*, 497.

28. Nepal, D.; Geckeler, K.E. Proteins and Carbon Nanotubes: Close Encounter in Water. *Small* **2007**, *3*, 1259–1265, doi:10.1002/smll.200600511.

29. Karajanagi, S.S.; Yang, H.; Asuri, P.; Sellitto, E.; Dordick, J.S.; Kane, R.S. Protein-assisted solubilization of single-walled carbon nanotubes. *Langmuir* **2006**, *22*, 1392–1395.

30. Joseph, D.; Tyagi, N.; Ghimire, A.; Geckeler, K.E. A direct route towards preparing pH-sensitive graphene nanosheets with anti-cancer activity. *RSC Adv.* **2014**, *4*, 4085–4093, doi:10.1039/C3RA45984E.

31. Bhattacharjee, S. DLS and zeta potential – What they are and what they are not? *J. Control. Release* **2016**, *235*, 337–351, doi:10.1016/J.JCONREL.2016.06.017.

32. Piella, J.; Bastús, N.G.; Puntes, V. Size-dependent protein–nanoparticle interactions in ctrate-stabilized gold nanoparticles: The emergence of the protein corona. *Bioconjug. Chem.* **2017**, *28*, 88–97, doi:10.1021/acs.bioconjchem.6b00575.

33. Boselli, L.; Polo, E.; Castagnola, V.; Dawson, K.A. Regimes of biomolecular ultrasmall nanoparticle interactions. *Angew. Chemie Int. Ed.* **2017**, *56*, 4215–4218, doi:10.1002/anie.201700343.

34. Bekdemir, A.; Stellacci, F. A centrifugation-based physicochemical characterization method for the interaction between proteins and nanoparticles. *Nat. Commun.* **2016**, *7*, 13121, doi:10.1038/ncomms13121.

35. Soldà, A.; Cantelli, A.; Di Giosia, M.; Montalti, M.; Zerbetto, F.; Rapino, S.; Calvaresi, M. C60@lysozyme: A new photosensitizing agent for photodynamic therapy. *J. Mater. Chem. B* **2017**, *1757*, 525–534, doi:10.1039/C7TB00800G.

36. Ge, C.; Du, J.; Zhao, L.; Wang, L.; Liu, Y.; Li, D.; Yang, Y.; Zhou, R.; Zhao, Y.; Chai, Z.; Chen, C. Binding of blood proteins to carbon nanotubes reduces cytotoxicity. *Proc. Natl. Acad. Sci. U. S. A.* **2011**, *108*, 16968–73, doi:10.1073/pnas.1105270108.

37. Walczyk, D.; Bombelli, F.B.; Monopoli, M.P.; Lynch, I.; Dawson, K.A. What the cell "Sees" in bionanoscience. *J. Am. Chem. Soc.* **2010**, *132*, 5761–5768, doi:10.1021/ja910675v.

38. Genheden, S.; Ryde, U. The MM/PBSA and MM/GBSA methods to estimate ligand-binding affinities. *Expert Opin. Drug Discov.* **2015**, *10*, 449–461, doi:10.1517/17460441.2015.1032936.

39. Wang, C.; Greene, D.; Xiao, L.; Qi, R.; Luo, R. Recent developments and applications of the MMPBSA method. *Front. Mol. Biosci.* **2017**, *4*, 87, doi:10.3389/fmolb.2017.00087.

40. Schneidman-Duhovny, D.; Inbar, Y.; Polak, V.; Shatsky, M.; Halperin, I.; Benyamini, H.; Barzilai, A.; Dror, O.; Haspel, N.; Nussinov, R.; Wolfson, H.J. Taking geometry to its edge: Fast unbound rigid (and hinge-bent) docking. *Proteins* **2003**, *52*, 107–112, doi:10.1002/prot.10397.

41. Andrusier, N.; Nussinov, R.; Wolfson, H.J. FireDock: Fast interaction refinement in molecular docking. *Proteins* **2007**, *69*, 139–159, doi:10.1002/prot.21495.

42. Kingsford, C.L.; Chazelle, B.; Singh, M. Solving and analyzing side-chain positioning problems using linear and integer programming. *Bioinformatics* **2005**, *21*, 1028–1039, doi:10.1093/bioinformatics/bti144.

43. Zhang, C.; Vasmatzis, G.; Cornette, J.L.; DeLisi, C. Determination of atomic desolvation energies from the structures of crystallized proteins. *J. Mol. Biol.* **1997**, *267*, 707–726, doi:10.1006/jmbi.1996.0859.

44. Case, D.A.; Darden, T.A.; Cheatham, E.T.; Simmerling, C.L.; Wang, J.; Duke, R.E.; Luo, R.; Walker, R.C.; Zhang, W.; Merz, K.M.; Roberts, B.; Hayik, S.; Roitberg, A.; Seabra, G.; Swails, J.; Götz, A.W.; Kolossváry, I.; F.Wong, K.; Paesani, F.; Vanicek, J.; M.Wolf, R.; Liu, J.; Wu, X.; Brozell, S.R.; Steinbrecher, T.; Gohlke, H.; Cai, Q.; Ye, X.; Wang, J.; Hsieh, M.-J.; Cui, G.; Roe, D.R.; Mathews, D.H.; Seetin, M.G.; Salomon-Ferrer, R.; C. Sagui, V.B.; Luchko, T.; Gusarov, S.; Kovalenko, A.; Kollman, P.A. (2012) AMBER 12, University of California, San Francisco.

45. Tsui, V.; Case, D.A. Theory and applications of the generalized born solvation model in macromolecular simulations. *Biopolymers* **2000**, *56*, 275–291, doi:10.1002/1097-0282(2000)56:4<275::AID-BIP10024>3.0.CO;2-E.

46. Calvaresi, M.; Bottoni, A.; Zerbetto, F. Thermodynamics of binding between proteins and carbon nanoparticles: The Case of C60@Lysozyme. *J. Phys. Chem. C* **2015**, *119*, 28077–28082, doi:10.1021/acs.jpcc.5b09985.

47. Calvaresi, M.; Furini, S.; Domene, C.; Bottoni, A.; Zerbetto, F. Blocking the passage: C60 geometrically clogs K + Channels. *ACS Nano* **2015**, *9*, 4827–4834, doi:10.1021/nn506164s.

48. Trozzi, F.; Marforio, T.D.; Bottoni, A.; Zerbetto, F.; Calvaresi, M. Engineering the fullerene-protein interface by computational design: The sum is more than its Parts. *Isr. J. Chem.* **2017**, *57*, 547–552, doi:10.1002/ijch.201600127.

49. Jonsson, M. Isoelectric spectra of native and base denatured crystallized swine pepsin. *Acta Chem. Scand.* **1972**, *26*, 3435–40.

50. Walsh, K.A. Trypsinogens and trypsins of various species. *Methods Enzymol.* **1970**, *19*, 41–63, doi:10.1016/0076-6879(70)19006-9.

51. Chen, Z.; Westerhoff, P.; Herckes, P. Quantification of C60 fullerene concentrations in water. *Environ. Toxicol. Chem.* **2008**, *27*, 1852, doi:10.1897/07-560.1.

52. Friedman, S.H.; DeCamp, D.L.; Sijbesma, R.P.; Srdanov, G.; Wudl, F.; Kenyon, G.L. Inhibition of the HIV-1 protease by fullerene derivatives: Model building studies and experimental verification. *J. Am. Chem. Soc.* **1993**, *115*, 6506–6509, doi:10.1021/ja00068a005.

53. Sijbesma, R.; Srdanov, G.; Wudl, F.; Castoro, J.A.; Wilkins, C.; Friedman, S.H.; DeCamp, D.L.; Kenyon, G.L. Synthesis of a fullerene derivative for the inhibition of HIV enzymes. *J. Am. Chem. Soc.* **1993**, *115*, 6510–6512, doi:10.1021/ja00068a006.

54. Marcorin, G.L.; Da Ros, T.; Castellano, S.; Stefancich, G.; Bonin, I.; Miertus, S.; Prato, M. Design and synthesis of novel [60]Fullerene Derivatives as Potential HIV Aspartic Protease Inhibitors. **2000**, *2*, 3955–3958, doi:10.1021/OL000217Y.

55. Schuster, D.I.; Wilson, S.R.; Schinazi, R.F. Anti-human immunodeficiency virus activity and cytotoxicity of derivatized buckminsterfullerenes. *Bioorg. Med. Chem. Lett.* **1996**, *6*, 1253–1256, doi:10.1016/0960-894X(96)00210-7.

56. Tokuyama, H.; Yamago, S.; Nakamura, E.; Shiraki, T.; Sugiura, Y. Photoinduced biochemical activity of fullerene carboxylic acid. *J. Am. Chem. Soc.* **1993**, *115*, 7918–7919, doi:10.1021/ja00070a064.

57. Iwashita, K.; Shiraki, K.; Ishii, R.; Tanaka, T.; Hirano, A. Liquid chromatographic analysis of the interaction between amino acids and aromatic surfaces using single-wall carbon nanotubes. *Langmuir* **2015**, *31*, 8923–8929, doi:10.1021/acs.langmuir.5b02500.

58. Calvaresi, M.; Hoefinger, S.; Zerbetto, F. Probing the structure of lysozyme-carbon-nanotube hybrids with molecular dynamics. *Chem. - A Eur. J.* **2012**, *18*, 4308–4313, doi:10.1002/chem.201102703.

59. Hirano, A.; Tanaka, T.; Kataura, H.; Kameda, T. Arginine side chains as a dispersant for individual single-

wall carbon nanotubes. *Chem. - A Eur. J.* **2014**, *20*, 4922–4930, doi:10.1002/chem.201400003.

60.   Hirano, A.; Kameda, T.; Wada, M.; Tanaka, T.; Kataura, H. Carbon nanotubes facilitate oxidation of cysteine residues of proteins. *J. Phys. Chem. Lett.* **2017**, *8*, 5216–5221, doi:10.1021/acs.jpclett.7b02157.

61.   Hirano, A.; Kameda, T.; Sakuraba, S.; Wada, M.; Tanaka, T.; Kataura, H. Disulfide bond formation of thiols by using carbon nanotubes. *Nanoscale* **2017**, *9*, 5389–5393, doi:10.1039/c7nr01001j.

62.   Deguchi, S.; Alargova, R.G.; Tsujii, K. Stable dispersions of fullerenes, c60 and c70, in water. preparation and characterization. *Langmuir* **2001**, *17*, 6013–6017, doi:10.1021/LA010651O.

63.   Tang, Y.J.; Ashcroft, J.M.; Chen, D.; Min, G.; Kim, C.-H.; Murkhejee, B.; Larabell, C.; Keasling, J.D.; Chen, F.F. Charge-associated effects of fullerene derivatives on microbial structural integrity and central metabolism. *Nano Lett.* **2007**, *7*, 754–760, doi:10.1021/nl063020t.

64.   Deryabin, D.G.; Efremova, L.V.; Vasilchenko, A.S.; Saidakova, E.V.; Sizova, E.A.; Troshin, P.A.; Zhilenkov, A.V.; Khakina, E.A. A zeta potential value determines the aggregate's size of penta-substituted [60]fullerene derivatives in aqueous suspension whereas positive charge is required for toxicity against bacterial cells. *J. Nanobiotechnology* **2015**, *13*, 50, doi:10.1186/s12951-015-0112-6.

65.   Deryabin, D.G.; Davydova, O.K.; Yankina, Z.Z.; Vasilchenko, A.S.; Miroshnikov, S.A.; Kornev, A.B.; Ivanchikhina, A.V.; Troshin, P.A. The Activity of [60]Fullerene derivatives bearing amine and carboxylic solubilizing Groups against *Escherichia coli*: A Comparative Study. *J. Nanomater.* **2014**, *2014*, 1–9, doi:10.1155/2014/907435.

66.   Tegos, G.P.; Demidova, T.N.; Arcila-Lopez, D.; Lee, H.; Wharton, T.; Gali, H.; Hamblin, M.R. Cationic fullerenes are effective and selective antimicrobial photosensitizers. *Chem. Biol.* **2005**, *12*, 1127–35, doi:10.1016/j.chembiol.2005.08.014.